Ultrafast dynamics of charge carrier photogeneration and geminate recombination in conjugated polymer:fullerene solar cells

J. G. Müller,* J. M. Lupton, and J. Feldmann
Lehrstuhl für Photonik und Optoelektronik, Department für Physik und CeNS, Ludwig-Maximilians-Universität, Amalienstrasse 54, 80799 München, Germany

U. Lemmer
Light Technology Institute, Universität Karlsruhe (TH) and CFN, Kaiserstrasse 12, 76131 Karlsruhe, Germany

M. C. Scharber† and N. S. Sariciftci
Linz Institute for Organic Solar Cells (LIOS), Physical Chemistry, Johannes Kepler University, Altenbergerstrasse 69, A-4040 Linz, Austria

C. J. Brabec
Konarka Technologies, Altenbergerstrasse 69, A-4040 Linz, Austria

U. Scherf
Fachbereich C, Universität Wuppertal, Gauss-Strasse 20, 42097 Wuppertal, Germany
(Received 29 May 2005; published 22 November 2005)

We investigate the nature of ultrafast exciton dissociation and carrier generation in acceptor-doped conjugated polymers. Using a combination of two-pulse femtosecond spectroscopy with photocurrent detection, we compare the exciton dissociation and geminate charge recombination dynamics in blends of two conjugated polymers, MeLPPP [methyl-substituted ladder-type poly(*p*-phenylene)] and MDMO-PPV [poly(2-methoxy,5-(3,7-dimethyloctyloxy)-1,4-phenylenevinylene], with the electron accepting fullerene derivative PCBM [1-(3-methoxycarbonyl)-propyl-1-phenyl-(6,6)C_{61}]. This technique allows us to distinguish between free charge carriers and Coulombically bound polaron pairs. Our results highlight the importance of geminate pair recombination in photovoltaic devices, which limits the device performance. The comparison of different materials allows us to address the dependence of geminate recombination on the film morphology directly at the polymer:fullerene interface. We find that in the MeLPPP:PCBM blend exciton dissociation generates Coulombically bound geminate polaron pairs with a high probability for recombination, which explains the low photocurrent yield found in these samples. In contrast, in the highly efficient MDMO-PPV:PCBM blend the electron transfer leads to the formation of free carriers. The anisotropy dynamics of electronic transitions from neutral and charged states indicate that polarons in MDMO-PPV relax to delocalized states in ordered domains within 500 fs. The results suggest that this relaxation enlarges the distance of carrier separation within the geminate pair, lowering its binding energy and favoring full dissociation. The difference in geminate pair recombination concurs with distinct dissociation dynamics. The electron transfer is preceded by exciton migration towards the PCBM sites. In MeLPPP:PCBM the exciton migration time decays smoothly with increasing PCBM concentration, indicating a trap-free exciton hopping. In MDMO-PPV:PCBM, however, the exciton migration time is found to show a threshold-like dependence on the PCBM concentration. This observation is explained by efficient interchain energy transfer in ordered MDMO-PPV domains in conjunction with exciton trapping.

DOI: 10.1103/PhysRevB.72.195208 PACS number(s): 78.47.+p, 72.80.Le, 72.20.Jv, 78.66.Qn

I. INTRODUCTION

Optoelectronic devices based on polymeric semiconductors are currently being commercialized as light emitting diodes (LEDs) for display applications. The understanding of charge carrier injection, transport, and recombination enabled the design of improved material systems, leading to organic LEDs with efficiencies comparable to those of the best inorganic LEDs.[1]

Organic photodetectors and solar cells rely on the inverse process, i.e., charge carrier generation from exciton dissociation. One of the most promising approaches for conjugated polymer photodetectors is based on a blend system consisting of a conjugated polymer acting as electron donor and fullerene molecules as acceptors.[2–4] Since the photoexcited neutral states (excitons) created in the polymer are dissociated at the interfaces between the two constituents of the blend, large interfacial areas of these bulk heterojunctions are crucial for an efficient charge transfer.[4] This can be achieved by functionalization of the fullerene providing a high solubility in organic solvents[5] and by a careful choice of solvents to optimize the film morphology.[6] In such samples the initial electron transfer can be as fast as 45 fs,[7] resulting in a quantum efficiency for charge photogeneration close

to unity and solar energy conversion efficiencies of 2.5–3.5%.[6,8]

The device performance, however, depends critically on the conditions of film preparation and on the specific materials used. Blend systems with comparable charge mobilities and similar efficiencies for electron transfer can show distinctly different efficiencies for photo-carrier generation.[9] As evident from photoluminescence quenching, in most blend systems of conjugated polymers with fullerenes the electron transfer to the fullerene is highly efficient. The predominant loss mechanism leading to insufficient photon-to-carrier conversion in some blends is thus the recombination of charge carriers subsequent to exciton dissociation. Carrier recombination has been studied intensively in polymer:fullerene blends, mostly by measuring the decay of the charge carrier population by transient absorption studies[2,10–14] or electron spin resonance,[15–17] and by the detection of magnetic-resonance-induced changes of the recombination rate.[18–20]

Recombination in polymer:fullerene blends is considered to be predominantly nongeminate, occurring after charge diffusion in the device. This is manifested by the dependence of the recombination rate on charge mobility,[21] charge trapping,[14] charge density,[13,17] and temperature.[22,23] Nongeminate recombination is strongly enhanced if charge transport toward the electrodes is hindered by domain boundaries between regions of electron donating and accepting material,[24] leading to a strongly morphology-dependent quantum efficiency.[6,25]

In neat conjugated polymer films geminate carrier recombination has been shown to reduce the photocurrent yield significantly. Intermediate states in between neutral excitons and fully separated charges (free polarons) are formed on an ultrafast time scale with a significant quantum yield.[26] Unless reexcited with a second laser pulse, these geminate polaron pairs were found to recombine with high probability.[27,28] In this work we address the question whether such bound intermediate states are also relevant in polymer:fullerene blends. We present evidence that in certain polymer:fullerene blends strong geminate recombination occurs. We show that in these blends geminate polaron pairs are formed *directly* after exciton dissociation and recombine subsequently, leading to a low quantum efficiency for photocurrent generation. While nongeminate recombination takes place after charge diffusion in the sample and therefore depends on macroscopic film properties as the size and shape of phase-separated regions and percolation, the geminate recombination investigated here occurs directly at the donor-acceptor boundary and depends on the energy landscape in direct vicinity thereof.

In our work we compare two high-quality conjugated polymers blended with functionalized fullerene 1-(3-methoxycarbonyl)-propyl-1-phenyl-(6,6)C_{61} (PCBM),[5] the methyl-substituted ladder-type poly(*p*-phenylene) (MeLPPP), and a poly(2-methoxy,5-(3,7-dimethyloctyloxy)-1,4-phenylenevinylene (MDMO-PPV). MeLPPP has been the subject of many photophysical studies and is a well-characterized conjugated polymer with a molecular weight of $M_w \approx 50\,000$ and a rigid ladder-type backbone. Cells using MDMO-PPV yield one of the highest photocurrent efficiency reported for polymer:fullerene based solar cells;[6] its molecular weight is about $M_w \approx 10^6$. Both polymers show an efficient electron transfer to the fullerene, leading to a strong photocurrent increase.[29,30] We estimated the yield for this process from photoluminescence quenching experiments, which show an exciton quenching of $\eta > 95\%$ upon adding 20% (by weight) PCBM to the conjugated polymer film. Despite a larger hole mobility for MeLPPP[31] as compared to MDMO-PPV,[32] we found in steady-state photocurrent measurements under illumination at $\lambda = 400$ nm that the photocurrent quantum efficiency is more than one order of magnitude larger for MDMO-PPV:PCBM than for MeLPPP:PCBM (0.1% for MeLPPP; 3% for MDMOPPV-based cells of 150 nm thickness with 20% PCBM by weight[33]).

In order to resolve the reason for the vastly different photocurrent yields, we employ a combination of ultrafast techniques with photocurrent measurements to investigate the dynamics of exciton dissociation, polaron generation, and geminate pair recombination with a sub-ps time resolution. The two-pulse photocurrent correlation technique[27,28,34,35] gives a more detailed picture of the charge photogeneration than purely optical experiments as it allows us to distinguish between bound polaron pairs and free polarons.[27,28] With a first femtosecond laser pulse we excite singlet intrachain excitons in a diode structure comprising the organic blend. A second tunable laser pulse with a photon energy below the HOMO-LUMO gap is applied after variable time delay and its effect on the photocurrent (PC) is measured. Changes of PC are either due to exciton depletion by the second pulse leading to a reduction of PC or due to the excitation of polaron pairs to higher lying states leading to a larger dissociation probability.

II. EXPERIMENT

In our experiments we use a regeneratively amplified femtosecond Ti:sapphire-laser with a repetition rate of 1 kHz and a pulse duration of 120 fs. Frequency-doubled pulses with a photon energy of $h\nu_1 = 3.1$ eV are used to excite the sample (Fig. 1). The tunable time-delayed second laser pulse is derived from an optical parametric amplifier pumped by the same system. In our main experiment we determine the relative photocurrent change $\Delta PC/PC$ induced by the second laser pulse. In contrast to conventional pump/probe experiments the fluence of the second laser pulse is about four times higher as compared to the excitation pulse. Due to its spectral position below the bandgap, however, direct excitation by the second pulse is an unlikely process. The photocurrent change is measured by a Lock-In amplifier with the *second* pulse train being modulated by a mechanical chopper at a frequency of 500 Hz, phase locked to the 1 kHz repetition rate of the laser system. For comparison the differential transmission ($\Delta T/T$) induced by the first pulse is also recorded. Here, the *first* laser pulse train is modulated by the chopper. The excitation density generated in the active layer by the 3.1 eV laser pulse is approximately 4×10^{17} cm^{-3}. For this density neither bimolecular annihilation nor amplified spontaneous emission affect the exciton lifetime.[36]

The organic blend system forms the active layer in a sandwich-type diode structure. A set of four samples of each

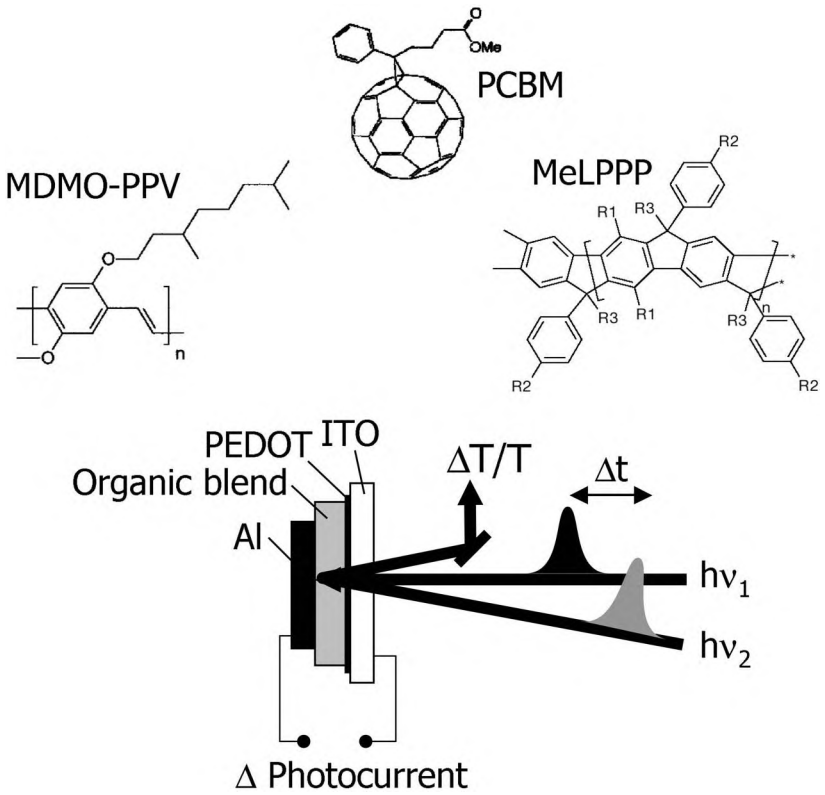

FIG. 1. Scheme of the experimental setup. A laser pulse with a photon energy of $h\nu_1 = 3.1$ eV excites the sample, followed by a second laser pulse with a tunable photon energy $h\nu_2$. Time-integrated changes of the photocurrent induced by the second pulse are measured as a function of time delay Δt. Additionally, the transmission change $\Delta T/T$ of the second pulse due to the excitation pulse is measured. The chemical structure of the organic materials used is also shown.

polymer with different amounts of PCBM between 0% and 60% by weight was prepared by spin coating the blend dissolved in toluene onto an indium-tin-oxide (ITO)-coated glass substrate. A thin layer of PEDOT [poly(3, 4-ethylenedioxythiophene)-poly(styrenesulfonate)] between ITO and polymer was introduced to improve the device performance. The thickness of the blend layer is between 150 and 200 nm. The diode structure was completed by evaporating an aluminum contact on top of the blend film. The reproducability of all measurements was checked with a second set of samples with identical parameters. The samples were stored in inert gas atmosphere. During all experiments the sample was mounted in a vacuum chamber with $p < 10^{-4}$ mbar to avoid sample degradation.

The optical properties of the polymers under investigation are shown in Fig. 2. The purely electronic 0-0 transition in MeLPPP is located at 2.7 eV. Due to the small inhomogeneous broadening in this polymer the absorption spectrum exhibits well-resolved vibronic replica at higher energies. In the case of MDMO-PPV both the absorption and the emission spectrum are subject to stronger inhomogeneous broadening. The fundamental optical transition sets in at approximately 2.1 eV.

In a first series of experiments the second laser pulse is tuned to the stimulated emission (SE) band. In MeLPPP strong SE is found at a photon energy of $h\nu_2 = 2.51$ eV.[37] In the case of MDMO-PPV we choose a photon energy $h\nu_2 = 1.97$ eV for this part of the experiments. For the second series of experiments addressing the role of polaron pairs the second laser pulse is spectrally located at the absorption bands of polarons. In MeLPPP we use $h\nu_2 = 1.9$ eV,[28,38] while $h\nu_2 = 1.78$ eV is chosen for MDMO-PPV (Refs. 39 and 40) (see Fig. 2).

III. RESULTS

A. MeLPPP blended with PCBM

We start the discussion with the results on MeLPPP blended with different amounts of PCBM. The differential $\Delta T/T$ transients measured at a probe energy of $h\nu_2 = 2.51$ eV are shown in Fig. 3(a). For all samples the population of photoexcited S_1 excitons leads to an initially strong stimulated emission resulting in a positive $\Delta T/T$-signal. The signal decay is dominated by the S_1-exciton lifetime of about

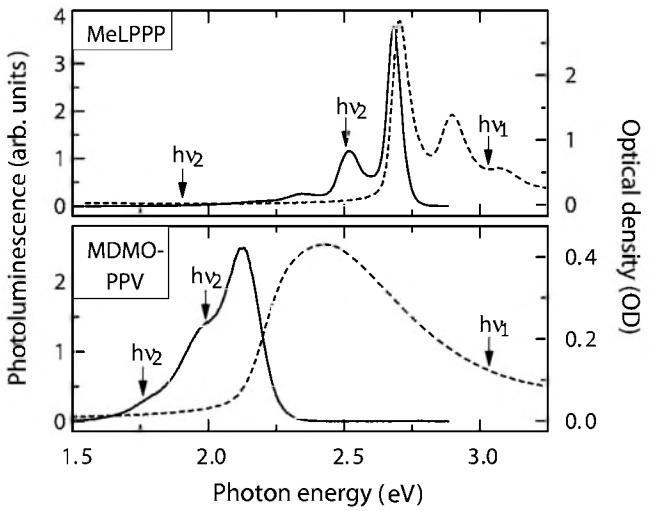

FIG. 2. Film spectra of absorption (dashed) and photoluminescence (solid line) of the polymers MeLPPP and MDMO-PPV. The spectral positions of the two applied laser pulses are indicated by arrows.

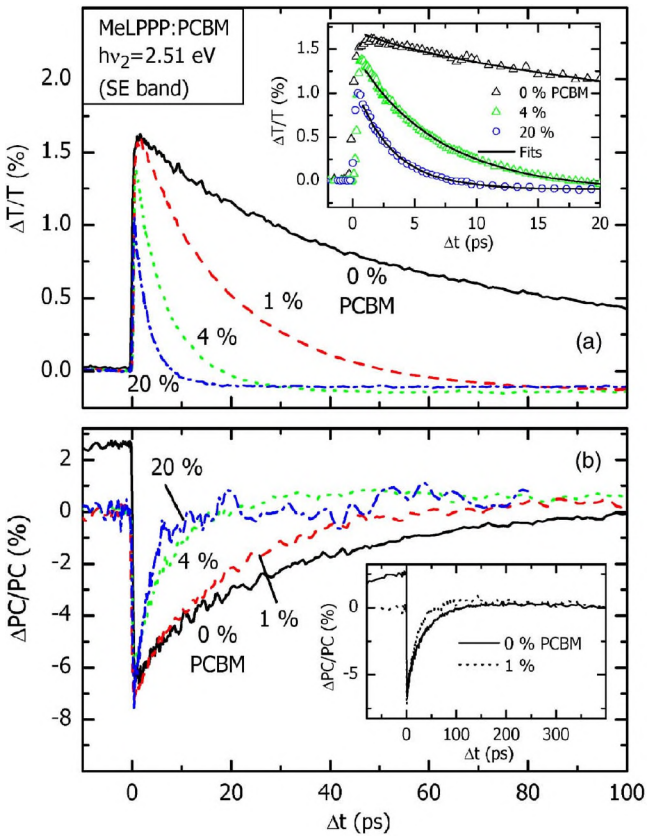

FIG. 3. (Color online) Time-resolved data of MeLPPP:PCBM samples with various PCBM concentrations. The second laser pulse has a photon energy of $h\nu_2$=2.51 eV, corresponding to the SE-band in MeLPPP. (a) The differential transmission of the second laser pulse. The inset shows data and fit curves according to Eq. (1) on a shorter timescale. (b) The relative photocurrent change induced by the second laser pulse. The inset shows $\Delta PC/PC$ of the neat MeLPPP sample and a sample doped with 1% PCBM on a longer time scale. The neat sample reveals a signal at negative time delay while this is absent for the doped sample.

80 ps in the case of the neat MeLPPP. As PCBM is added the lifetime is gradually reduced down to ≈3 ps at a PCBM concentration of 20%. This behavior is explained by the random walk of photogenerated excitons in MeLPPP. When a site close to a PCBM molecule is reached, rapid electron transfer leads to a dissociation of the S_1 exciton.[29,41] Thus quenching becomes gradually faster as the density of PCBM-related dissociation sites is increased.

The samples containing PCBM exhibit a small negative $\Delta T/T$ at large time delays. This is attributed to a weak photo-induced absorption (PIA) from charged species, generated by electron transfer to the PCBM.

We determine the exciton dissociation time by an exponential fit accounting for both SE and PIA,

$$\frac{\Delta T}{T}(t) = A_{\mathrm{SE}} \exp[-(t/\tau)^{\beta} - t/\tau_{\mathrm{diss}}] + A_{\mathrm{PIA}}(1 - \exp(-t/\tau_{\mathrm{diss}})). \tag{1}$$

The first term with the amplitude A_{SE} accounts for the decay of the SE signal. The behavior of the neat polymer is described using a stretched exponential with time constant τ and exponent β; the dissociation time constant τ_{diss} is set to infinity in this case. For the samples containing PCBM, the dissociation is switched on by fitting τ_{diss} while leaving τ, β fixed. The second term in Eq. (1) accounts for the weak PIA caused by charge carriers. As shown in the inset of Fig. 3(a), an excellent fit to the neat polymer data is achieved for τ =61 ps, β=0.75. The subsequent fit to the samples containing 4% and 20% PCBM yields $\tau_{\mathrm{diss,4\%}}$=8.3 ps and $\tau_{\mathrm{diss,20\%}}$ =3.4 ps, respectively.

The amplitude of $\Delta T/T$ slightly decreases with increasing PCBM concentration. The PCBM absorbs part of the pump light and reduces the concentration of the polymer. Both effects diminish the polymer absorption, leading to a reduced SE signal. Since these effects account for the total amplitude reduction observed, we conclude that electron transfer on time scales shorter than the temporal resolution of the experiment does not occur, for this would further reduce the exciton population. This notion is confirmed by results discussed in the next section.

The relative photocurrent changes ($\Delta PC/PC$) induced by the second laser pulse with a photon energy of $h\nu_2$ =2.51 eV are shown in Fig. 3(b). The negative $\Delta PC/PC$ signal has a decay time similar to the SE signal in Fig. 3(a), therefore it is attributed to the depletion of S_1 excitons induced by the second laser pulse. Since excitons are precursor states for charge carrier generation, stimulated deactivation leads directly to a reduction of the photocurrent.[28,34] In agreement with this scenario the decay of the $\Delta PC/PC$ signal is accelerated when PCBM is added to the polymer.

In the case of the neat polymer sample an additional $\Delta PC/PC$ signal at negative time delays is present [see also inset of Fig. 3(b)]. Residual ground-state absorption of the second laser pulse at $h\nu$=2.51 eV (180 meV below the fluorescence maximum), possibly due to anti-Stokes excitation with the aid of a molecular vibration,[42] leads to the formation of excitons by the second laser pulse. These can undergo bimolecular annihilation (BMA) with the excitons created by the first laser pulse, subsequently creating highly excited excitons with high dissociation probability.[43,44] In the presence of PCBM the relative contribution of BMA to the photocurrent becomes negligible as electron transfer to the acceptor by far dominates the photocarrier generation. The signature of BMA in the $\Delta PC/PC$ disappears completely.

The amplitude of $\Delta PC/PC$ is unaffected by the presence of PCBM molecules. This is in agreement with the conclusion drawn from the discussion of the amplitude in $\Delta T/T$ measurements, where an electron transfer on time scales shorter than the time resolution of the setup was ruled out. Here, changes of the optical density due to a reduced MeLPPP concentration upon adding PCBM do affect both PC and ΔPC equally, thus the amplitude of the relative change $\Delta PC/PC$ remains unmodified.

In order to monitor the population of charge carriers in the sample, i.e., polarons and polaron pairs, we tune the second laser pulse to the absorption band of charge carriers at a photon energy of $h\nu_2$=1.9 eV.[28,38] The $\Delta T/T$ data taken at this photon energy are shown in Fig. 4(a). The neat polymer sample shows PIA with a decay time corresponding to the singlet exciton lifetime discussed above. We conclude that

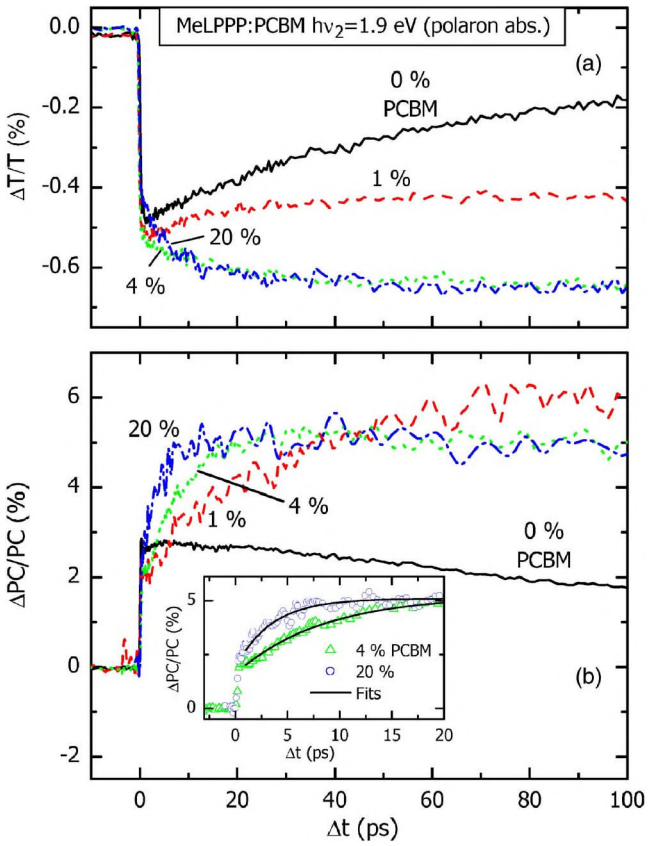

FIG. 4. (Color online) Time-resolved data of MeLPPP:PCBM samples with various PCBM concentrations. The second laser pulse has a photon energy of $h\nu_2$=1.9 eV, corresponding to the polaron absorption band in MeLPPP. (a) The differential transmission of the second laser pulse. (b) The relative photocurrent change induced by the second laser pulse. The inset shows data and fit curves according to Eq. (2) on a shorter timescale.

the PIA signal is rather dominated by $S_n \leftarrow S_1$ excited state absorption than by PIA due to charged species. At increased PCBM concentration, however, the signal shows a strong and long-living PIA. Particularly at high PCBM concentrations, the formation of this signal can be directly observed. The buildup time corresponds approximately to the decay time of excitons as extracted from Fig. 3. We conclude that this long-living PIA signal, appearing faster and stronger as the PCBM-concentration is increased, is caused by the buildup of charged species as a result of electron transfer to the PCBM. An increase of the PCBM concentration from 4% to 20% leaves the amplitude of the PIA unchanged. This reflects the fact that already at 4% PCBM nearly all photoexcitations undergo electron transfer to the PCBM.

Free polarons and Coulombically bound polaron pairs give rise to similar photoinduced absorption bands and cannot be distinguished in transient absorption studies. The $\Delta PC/PC$ signal measured at this photon energy allows us to disentangle these two species, as the PC arises primarily from free carriers. The photocurrent changes $\Delta PC/PC$ induced by the second laser pulse are shown in Fig. 4(b). In all samples the second laser pulse leads to an enhanced photocurrent. As recently shown for neat MeLPPP samples, polaron pairs can be reexcited into states with higher dissociation probability, leading to an increased photocurrent yield.[28] From our data we conclude that reexcitation of polaron pairs also leads to an increased photocurrent in samples containing PCBM. Although in this case exciton dissociation by electron transfer to the PCBM is efficient, the hole on a MeLPPP segment and the electron on the PCBM molecule remain Coulombically bound to each other and form a polaron pair with a high probability for recombination. Similar to the case of the neat polymer, the 1.9 eV photon from the second laser pulse supplies the necessary energy to reexcite polaron pairs to a state with higher dissociation probability. Since there is no significant C_{60} anion absorption at 1.9 eV,[45] the second laser pulse is absorbed by the hole on the MeLPPP, enhancing its probability to escape the attractive Coulomb potential of the PCBM anion and thereby reducing charge recombination.

The decay times of $\Delta PC/PC$ range from about 300 ps in the neat MeLPPP sample to much larger values in samples containing PCBM. The large energy difference of the LUMO levels of polymer and PCBM of about 1 eV (Refs. 4 and 46) supresses the electron back transfer from PCBM to the polymer. For various conjugated polymer:fullerene blends recombination times of microseconds and longer have been reported.[11,15] In agreement with those observations the lifetime of the MeLPPP:PCBM polaron pairs exceeds the time scale of our measurements in Fig. 4. In neat MeLPPP, however, the polaron pair is almost isoenergetic with the excitonic state.[47] Thus recombination of the polaron pair in the neat polymer is more probable, resulting in a shorter polaron pair lifetime.

The rise time of the $\Delta PC/PC$ signal corresponds to the formation time of polaron pairs. All samples exhibit an ultrafast rise of the $\Delta PC/PC$ signal within the pump-pulse duration, which has been attributed to the ultrafast formation of intrachain polaron pairs in MeLPPP.[28] In samples containing PCBM an additional rise of the $\Delta PC/PC$ signal occurs due to the time-delayed electron transfer. This rise time shortens with increasing PCBM concentration and corresponds to the migration time required for the exciton to reach a site next to a PCBM molecule, which is probed by SE depletion in Fig. 3. Within the first few tens of picoseconds any decay of the photocurrent signal can be neglected and we describe the rise of $\Delta PC/PC$ by a single exponential term,

$$\frac{\Delta PC}{PC}(t) = A_{\Delta PC}(1 - \exp(-t/\tau_{\text{diss}})) + \Delta PC_{t=0}, \qquad (2)$$

where τ_{diss} is the time constant for the time-delayed exciton dissociation, $A_{\Delta PC}$ is the amplitude, and the offset $\Delta PC_{t=0}$ accounts for the ultrafast rise of $\Delta PC/PC$ within the experimental time resolution. An excellent fit is obtained for the samples with 4% and 20% PCBM by using the exciton dissociation times as determined above in the discussion of Fig. 3(a), $\tau_{\text{diss},4\%}$=8.3 ps and $\tau_{\text{diss},20\%}$=3.4 ps, respectively. The inset in Fig. 4(b) shows data and fit curves.

We conclude that the polaron pairs probed in Fig. 4 are formed directly after electron transfer to the PCBM, and therefore have to be geminate pairs.

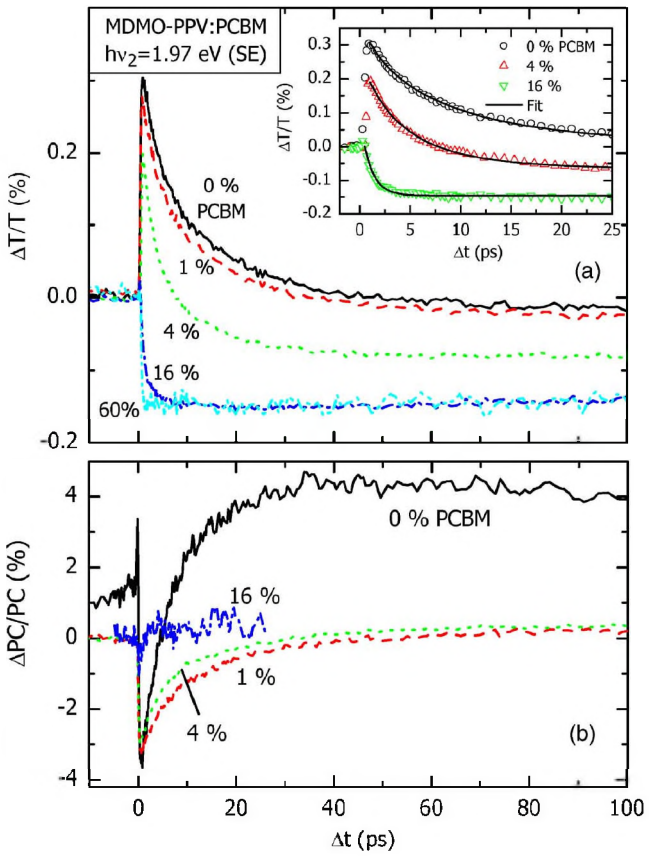

FIG. 5. (Color online) Time-resolved data of MDMO-PPV:PCBM samples with various PCBM concentrations. The second laser pulse has a photon energy of $h\nu_2=1.97$ eV. (a) The differential transmission of the second laser pulse. The inset shows the data with fit curves according to Eq. (1) on a shorter time scale. (b) The relative photocurrent change induced by the second laser pulse.

The amplitude of the relative photocurrent increase $\Delta PC/PC$, however, is almost identical for all PCBM concentrations. Apparently, the probability for geminate recombination is virtually independent of the PCBM concentration and any related changes in film morphology. This behavior is not surprising, since the geminate pair cannot leave the polymer:PCBM domain boundary, implying that geminate recombination does not depend on the domain size of the individual constituents of the blend as long as it exceeds the spatial extension of the geminate pair.

B. MDMO-PPV blended with PCBM

In the following section the results obtained on samples of the conjugated polymer MDMO-PPV blended with PCBM are described and compared with the results obtained for MeLPPP:PCBM.

In Fig. 5(a) the differential transmission signal after pumping with femtosecond pulses at 3.1 eV is shown for MDMO-PPV blended with different amounts of the electron acceptor PCBM. The probe photon energy is tuned to the first vibronic side band observed in the photoluminescence spectrum at $h\nu_2=1.97$ eV (see Fig. 2), thereby enabling SE and hence depletion of the excited state.

The transients of MDMO-PPV samples with a PCBM concentration of up to 4% show a positive $\Delta T/T$ signal due to SE. As observed for the MeLPPP:PCBM samples, the decay times become shorter with increasing PCBM concentration. In contrast to the MeLPPP:PCBM samples, however, the amplitude undergoes a significant decrease by $\approx$30% at 4% PCBM, indicating instantaneous electron transfer to the PCBM within the experimental time resolution of 300 fs. At a PCBM concentration of 16% the contribution from SE in the $\Delta T/T$ signal has almost vanished [inset of Fig. 5(a)]. We estimate that in this sample roughly 90% of the excitons dissociate within 300 fs.

At increased PCBM concentrations a long-living PIA signal appears in the $\Delta T/T$ transients. Like in MeLPPP:PCBM, this signal is characteristic for the generation of charged species due to the electron transfer from the photoexcited polymer to the PCBM molecules. The amplitude is the same for fullerene concentrations of 16% and 60%, indicating that the efficiency for electron transfer approaches unity for these blends.

Using Eq. (1) we calculate the exciton dissociation rate for the samples with 4% and 16% PCBM. The fit curves are shown in the inset of Fig. 5(a). For the neat MDMO-PPV sample we use $\tau=7.1$ ps and $\beta=0.71$. Leaving these parameters fixed, we obtain a dissociation time of $\tau_{\mathrm{diss},4\%}=9.9$ ps for the sample with 4% PCBM. The sample with 16% PCBM shows a much faster dissociation of only $\tau_{\mathrm{diss},16\%}=1.1$ ps. Compared to the respective numbers obtained in the previous section on MeLPPP:PCBM samples, the dissociation in MDMO-PPV:PCBM is slower at a low PCBM concentration of 4%, but much faster at high PCBM concentrations above 16%.

The observation of a strong PIA in MDMO-PPV at the center of the first vibronic sideband of the photoluminescence competing with SE is in contrast with the behavior in MeLPPP. Due to the larger inhomogeneous broadening in MDMO-PPV, the SE band of the exciton overlaps with the PIA band of the charged species. The resulting superposition of positive and negative contributions to the $\Delta T/T$ signal also determines the behavior with the second pulse tuned to $h\nu_2=1.78$ eV, as discussed in more detail below. At this probe energy the SE turns out to be weaker than the PIA, so that the differential transmission signal is dominated by PIA.

The superposition of SE by excitons and PIA by charges is also evident in the $\Delta PC/PC$ data. As shown in Fig. 5(b), in the neat MDMO-PPV sample the second laser pulse at $h\nu_2=1.97$ eV induces a pronounced, initially negative signal due to depletion of the exciton population. In the same transient, a strong photocurrent increase appears at $\Delta t>6$ ps. The lifetime of the positive $\Delta PC/PC$ signal is about 300 ps, exceeding by far the stimulated emission lifetime in MDMO-PPV at this photon energy. As described above for the MeLPPP sample, the long-living photocurrent enhancement is assigned to the reexcitation of polaron pairs by the second laser pulse, increasing the dissociation yield of the Coulombically bound pairs. In analogy to the corresponding dataset obtained for MeLPPP in Fig. 3(b), the $\Delta PC/PC$ signal of the neat MDMO-PPV shows a small decay at negative time-delay, which is a result of residual ground-state absorption at the photon energy of the second laser pulse at $h\nu_2=1.97$ eV.

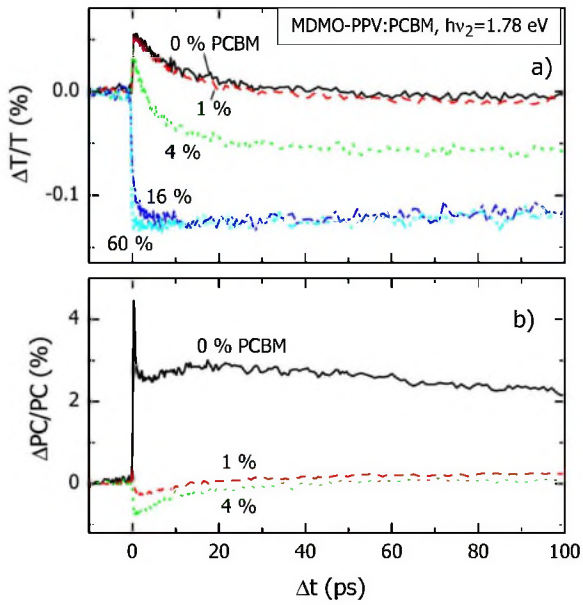

FIG. 6. (Color online) Time-resolved data of MDMO-PPV:PCBM samples with various PCBM concentrations. The second laser pulse has a photon energy of $h\nu_2=1.78$ eV. (a) The differential transmission of the second laser pulse. (b) The relative photocurrent change induced by the second laser pulse.

Since the electron transfer itself is as fast as 45 fs,[7] the decay of the stimulated depletion signal observed in Fig. 5(b) is given by the exciton diffusion time that is required to reach a site close to a PCBM molecule. In analogy to the $\Delta T/T$ data in Fig. 5(a), the photocurrent depletion signal becomes only slightly faster when up to 4% PCBM is added, implying an exciton diffusion time comparable to the exciton lifetime in neat MDMO-PPV. At a PCBM concentration of 16%, however, the amplitude of the photocurrent depletion signal is drastically reduced, showing that about 90% of the excitons dissociate within the experimental time resolution of 300 fs. This observation is in full agreement with the quantitative analysis of the corresponding $\Delta T/T$ data [Fig. 5(a) and discussion]. Since an increase of the PCBM concentration from 4% to 16% corresponds to a mere 40% decrease of the average PCBM distance, the sudden acceleration of exciton dissociation is surprising and in striking contrast to the behavior observed at the MeLPPP:PCBM samples, where the exciton dissociation time decreases smoothly with increasing PCBM concentration.

Due to the less pronounced SE at a probe energy of $h\nu_2=1.78$ eV, the photocurrent enhancement induced by the second laser pulse can be observed more clearly in Fig. 6(b). At this spectral position the photocurrent depletion by SE is weak and only results in a small dip in the transient for the neat polymer film at around $\Delta t=5$ ps. The dominant contribution to the photocurrent modulation is positive due to facilitated carrier separation. Surprisingly, the second pulse enhances the photocurrent of the neat MDMO-PPV film by 5% although no PIA is detected in the corresponding $\Delta T/T$ data in Fig. 6(a). We conclude that the probability of dissociation of polaron pairs upon absorption of a 1.78 eV photon by far exceeds the dissociation probability of a neutral exciton in the neat MDMO-PPV sample. Similar to the case of MeLPPP the fast initial rise of $\Delta PC/PC$ at $\Delta t=0$ indicates that a portion of the excitons form polaron pairs in MDMO-PPV within 300 fs.

The $\Delta PC/PC$ transients are drastically changed upon adding PCBM. Even a small PCBM content of only 1% completely suppresses the photocurrent enhancement. Only the negative $\Delta PC/PC$ signal due to stimulated exciton depletion remains. This is just the opposite to the observations in MeLPPP:PCBM-blends, where the positive $\Delta PC/PC$ signal even increases in strength upon blending with PCBM. We conclude that in the MDMO-PPV:PCBM samples no stable polaron pairs are formed after electron transfer to the PCBM, i.e., geminate pairs consisting of a hole located on the MDMO-PPV and an electron on the PCBM fully dissociate spontaneously. Consequently, the second laser pulse cannot increase the photocurrent any further. This scenario is in agreement with the vanishing magnetic-resonance effect on the photocurrent at increased PCBM concentrations reported recently on MDMO-PPV:PCBM solar cells.[20]

IV. DISCUSSION

The photocurrent quantum yield in the MDMO-PPV:PCBM samples is well below one ($\eta_{PC}\approx 0.03$ for 20% PCBM), implying that strong charge recombination occurs. The reexcitation of polarons with the second laser pulse, however, leads to a large photocurrent increase in neat MDMO-PPV only, while it has no effect on the photocurrent in the MDMO-PPV:PCBM blend even at low PCBM concentrations. This can be explained by the different nature of geminate and nongeminate recombination. Nongeminate recombination occurs after charge diffusion in the device and competes with charge extraction at the electrodes. Although the second laser pulse may increase the charge mobility by releasing charge carriers from deep traps, it does not affect the nongeminate recombination yield since nongeminate recombination and charge extraction depend on the mobility in the same way.[23] Geminate recombination, however, can be reduced by the second laser pulse by facilitating to surmount the attractive Coulomb potential of the counterion.

Consequently, our results show that in the MDMO-PPV:PCBM samples geminate recombination occurs only in the absence of PCBM. We can exclude geminate recombination of charges created by electron transfer from MDMO-PPV to PCBM. In contrast, charge pairs created by exciton dissociation in the material system MeLPPP:PCBM apparently recombine geminately with a high probability. This results in a low photocurrent quantum yield on the one hand; on the other hand, however, it leads to a strong enhancement in photocurrent upon excitation of polaron pairs with a second laser pulse.

Different explanations for the distinct behavior of the two material systems are conceivable: (*i*) In a recent theoretical study the dependence of the geminate recombination rate on the effective mass of the hole in the polymer was discussed.[48] However, we are not aware of any indication for a much larger effective mass in MeLPPP as compared to

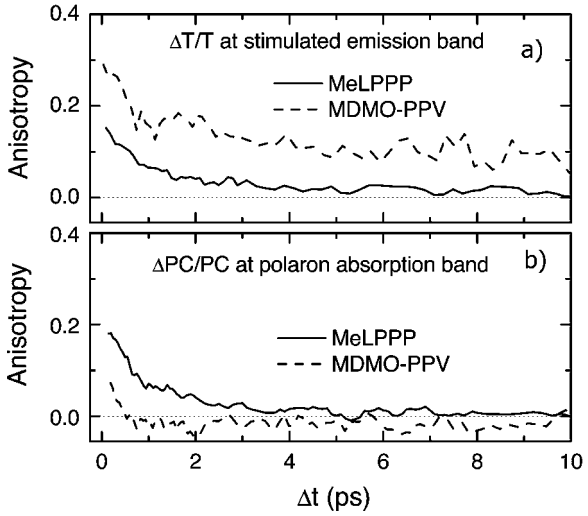

FIG. 7. (a) Anisotropy of $\Delta T/T$ in the neat polymer films, measured in the SE band (MeLPPP: $h\nu_2=2.51$ eV, MDMO-PPV: $h\nu_2=1.97$ eV). (b) Anisotropy of $\Delta PC/PC$ in neat polymer films, measured in the polaron absorption band of (MeLPPP: $h\nu_2=1.9$ eV, MDMO-PPV: $h\nu_2=1.78$ eV).

MDMO-PPV. (*ii*) A recent investigation of Monte Carlo simulations of photocurrent generation in conjugated-polymer:fullerene blends proposed that disorder within the polymer system facilitates the surmounting of the mutual Coulomb attraction of a geminate pair.[49] This model agrees well with our observations, since the site disorder in MeLPPP is much smaller than in MDMO-PPV (see absorption spectra in Fig. 2). (*iii*) The probability for geminate recombination of a charge pair is directly related to the shape of the energy landscape for the charge carriers, determined by the external field, the Coulombic interaction with the counter charge, and the spatial and energetic site distribution. The latter is largely influenced by the film morphology, since interchain interactions in ordered regions generally lead to a reduced site energy.[50] We note that an important difference between PPVs and LPPPs is the tendency of PPVs to form aggregates even from single molecules[51] whereas MeLPPP does not show any significant aggregation, neither on a single-molecule level[51] nor in films.[52]

In order to examine the film morphology on the molecular scale, we performed measurements of the ultrafast anisotropy dynamics of the $\Delta T/T$- and $\Delta PC/PC$-signals. The anisotropy r is calculated according to $r=(S_\parallel-S_\perp)/(S_\parallel+2S_\perp)$, where $S_\parallel$ and $S_\perp$ are the signals obtained for parallel and perpendicular polarized laser pulses, respectively. The results confirm that the two polymers form films with very distinct morphologies, which directly affect the microscopic interface between molecular donor and acceptor species. Figure 7(a) shows the anisotropy of the stimulated emission measured for the neat polymer films. The initial anisotropy of the SE of MeLPPP observed in Fig. 7(a) reaches only $r=0.15$, far less than the theoretical value for a disordered ensemble of linear transition dipole moments of $r_{\text{theo}}=0.4$.[53] A very recent single molecule study has shown that the transition dipole moments of MeLPPP are highly anisotropic, both in excitation and in emission.[54] The low anisotropy observed here therefore results from ultrafast exciton hopping between segments of different orientation, which can also occur efficiently within one single molecule.[54]

The SE of MDMO-PPV has an initial anisotropy of $r=0.3$, twice as large as the corresponding value for MeLPPP. Recent calculations of the exciton hopping in polyindenofluorene films predicted that interchain hopping between parallel chain segments is about one order of magnitude faster than intrachain hopping.[55] We conclude that the initial exciton migration steps in MDMO-PPV are preferentially of an interchain type and occur between stacked conjugated segments with parallel orientation, thereby maintaining the polarization of the transition dipole moment.

The different chain packing in films of the two conjugated polymers is also evident from the anisotropy of the photocurrent enhancement observed when polaron pairs in the polymer are reexcited with the second laser pulse, shown in Fig. 7(b). Here the signal represents the anisotropy of the transition dipole moment for excitation of polarons. In the case of MeLPPP the initial anisotropy of polarons is $r=0.2$, exceeding the corresponding value for excitons [Fig. 7(a)]. This observation was recently assigned to polarons created in an ultrafast on-chain exciton dissociation process.[28] In contrast, the initial anisotropy of $r=0.08$ found for polarons in MDMO-PPV is very low. Since the high anisotropy of excitons indicated the presence of ordered domains in this polymer, the low anisotropy of polarons is surprising. Despite the low initial value of r the anisotropy decays fast within about 500 fs and levels off at a slightly negative value. This indicates that the transition dipole moment involved in the excitation of polarons in MDMO-PPV is initially oriented along the polymer backbone, but becomes slightly perpendicular to the backbone within less than 1 ps. We suggest that close chain packing in ordered domains of the MDMO-PPV film leads to the delocalization of polarons over stacked polymer chains. Accordingly, the rapid decrease of anisotropy represents the relaxation of the polaron to an energetically favorable state, delocalized over several chains in an ordered domain. Interchain interactions leading to more delocalized polarons may result in a larger distance between the geminate charges, lowering their binding energy and reducing geminate recombination.

The presence of ordered domains in MDMO-PPV also explains our observation that the exciton lifetime in MDMO-PPV remains almost unchanged if small amounts (up to 4%) of PCBM are added to MDMO-PPV, but suddenly drops by an order of magnitude when the concentration is increased to 16% (Fig. 5): Those aggregates of MDMO-PPV that contain PCBM are quenched almost instantaneously due to fast interchain energy transfer, whereas aggregates free of PCBM remain rather unaffected since the exciton is trapped within the aggregate.

Films of MeLPPP, however, exhibit no significant aggregation[52] and show a much smaller inhomogeneous broadening which reduces exciton trapping, enabling exciton migration throughout the entire exciton lifetime.[56] The absence of trapping leads to the observed smooth decrease of exciton lifetime as the PCBM concentration is increased. The notion of a larger exciton migration range in MeLPPP due to less trapping is supported by the observation that in MeLP-

PP:PCBM a PCBM concentration of 4% leads to almost complete exciton quenching, as can be seen from the saturation of charge carrier density with increasing PCBM content in Fig. 4(a). In MDMO-PPV:PCBM, however, 4% PCBM leads to quenching of only about half of all excitons [Fig. 6(a)].

V. SUMMARY

We compared the dynamics of exciton dissociation and geminate charge recombination in two distinct polymer-:fullerene blend photodiodes, using MeLPPP:PCBM and MDMO-PPV:PCBM as active layers. Probing the SE of photogenerated excitons and its effect on the photocurrent yield, we measured the exciton migration time, i.e., the time until a site next to a PCBM is reached and dissociation occurs. A much stronger dependence of the migration time on the PCBM density is found for MDMO-PPV:PCBM, indicating that here exciton migration is much faster on short distances, but slower than in MeLPPP:PCBM on distances exceeding a few nanometers. This is explained by close stacking of chain segments in films of MDMO-PPV enabling fast interchain energy transfer, concomitant with excitation trapping due to strong disorder.

Measuring the photocurrent change induced by a second laser pulse tuned to the absorption of charge carriers in the polymers, we find a strong photocurrent enhancement within 300 fs after initial photoexcitation for both polymers, if no PCBM is added. The signal is attributed to the formation of geminate polaron pairs with a high probability of recombination; the second laser pulse excites the polaron pairs, facilitating the escape from the mutual Coulomb attraction and leading to complete dissociation.

The presence of PCBM enhances the photocurrent increase in MeLPPP:PCBM due to the enhanced formation of polaron pairs, which in this case are formed by a hole on the polymer chain and the PCBM anion. We conclude that this type of polaron pair also suffers from geminate recombination with a high probability. In MDMO-PPV:PCBM, however, the photocurrent increase due to photoinduced geminate pair dissociation disappears as soon as low concentrations of PCBM are present. Apparently, after exciton dissociation at the MDMO-PPV:PCBM domain boundary the mutual attraction of the hole on the polymer and the PCBM anion is easily overcome without the help of a second laser pulse, i.e., no polaron pairs are formed.

Our results show that geminate charge recombination significantly reduces the photocurrent yield in certain conjugated polymer:fullerene blends. As opposed to nongeminate recombination occurring after charge migration in the device, geminate recombination takes place at or in the direct vicinity of the location of exciton dissociation and therefore depends on the very local structure at the polymer:fullerene domain boundary.

The anisotropy measurements provide a link between the distinctly different dissociation and recombination dynamics in the two polymer blends and the film morphology. The anisotropy dynamics reveal ordered domains in MDMO-PPV and indicate a fast relaxation of polarons towards delocalized states in those domains. We conclude that in MDMO-PPV:PCBM blends the relaxation of the hole-polaron from the polymer:fullerene interface towards ordered domains enlarges the distance between geminate charge carriers, thereby reducing the binding energy and the probability for geminate recombination.

ACKNOWLEDGMENTS

We thank W. Stadler and A. Helfrich for excellent technical support and acknowledge helpful discussions with E. Frankevich. The work was supported financially by the DFG through the Sonderforschungsbereich (SFB) 377 and the Gottfried-Wilhelm-Leibniz-award.

*Present address: Light Technology Institute, Universität Karlsruhe, Kaiserstrasse 12, 76131 Karlsruhe, Germany.

†Present address: Konarka Technologies, Altenbergerstrasse 69, A-4040 Linz, Austria.

[1] J. N. Bardsley, IEEE J. Sel. Top. Quantum Electron. **10**, 3 (2004).

[2] N. S. Sariciftci, L. Smilowitz, A. J. Heeger, and F. Wudl, Science **258**, 1474 (1992).

[3] J. J. M. Halls, K. Pichler, R. H. Friend, S. C. Moratti, and A. B. Holmes, Appl. Phys. Lett. **68**, 3120 (1996).

[4] C. J. Brabec, N. S. Sariciftci, and J. C. Hummelen, Adv. Funct. Mater. **11**, 15 (2001).

[5] J. C. Hummelen, B. W. Knight, F. Lepeq, F. Wudl, J. Yao, and C. L. Wilkins, J. Org. Chem. **60**, 532 (1995).

[6] S. E. Shaheen, C. J. Brabec, N. S. Sariciftci, F. Padinger, T. Fromherz, and J. C. Hummelen, Appl. Phys. Lett. **78**, 841 (2001).

[7] C. J. Brabec, G. Zerza, G. Cerullo, S. De Silvestri, S. Luzzati, J. C. Hummelen, and S. Sariciftci, Chem. Phys. Lett. **340**, 232 (2001).

[8] F. Padinger, R. S. Rittberger, and N. S. Sariciftci, Adv. Funct. Mater. **13**, 85 (2003).

[9] T. Fromherz, F. Padinger, D. Gebeyehu, C. Brabec, J. C. Hummelen, and N. S. Sariciftci, Sol. Energy Mater. Sol. Cells **63**, 61 (2000).

[10] B. Kraabel, D. McBranch, N. S. Sariciftci, D. Moses, and A. J. Heeger, Phys. Rev. B **50**, 18543 (1994).

[11] C. J. Brabec, V. Dyakonov, N. S. Sariciftci, W. Graupner, G. Leising, and J. C. Hummelen, J. Chem. Phys. **109**, 1185 (1998).

[12] S. V. Frolov, P. A. Lane, M. Ozaki, K. Yoshino, and Z. V. Vardeny, Chem. Phys. Lett. **286**, 21 (1998).

[13] I. Montanari, A. F. Nogueira, J. Nelson, J. R. Durrant, C. Winder, M. A. Loi, N. S. Sariciftci, and C. Brabec, Appl. Phys. Lett. **81**, 3001 (2002).

[14] A. F. Nogueira, I. Montanari, J. Nelson, J. R. Durrant, C. Winder, and N. S. Sariciftci, J. Phys. Chem. B **107**, 1567 (2003).

[15] L. Smilowitz, N. S. Sariciftci, R. Wu, C. Gettinger, A. J. Heeger, and F. Wudl, Phys. Rev. B **47**, 13835 (1993).

[16] R. A. J. Janssen, J. Jansen, J. vanHaare, and E. W. Meijer, Adv. Mater. (Weinheim, Ger.) **8**, 494 (1996).
[17] N. A. Schultz, M. C. Scharber, C. J. Brabec, and N. S. Sariciftci, Phys. Rev. B **64**, 245210 (2001).
[18] E. L. Frankevich, A. A. Lymarev, I. Sokolik, F. E. Karasz, S. Blumstengel, R. H. Baughman, and H. H. Horhold, Phys. Rev. B **46**, 9320 (1992).
[19] P. A. Lane, J. Shinar, and K. Yoshino, Phys. Rev. B **54**, 9308 (1996).
[20] M. C. Scharber, N. A. Schultz, N. S. Sariciftci, and C. J. Brabec, Phys. Rev. B **67**, 085202 (2003).
[21] C. J. Brabec, C. Winder, M. C. Scharber, N. S. Sariciftci, J. C. Hummelen, M. Svensson, and M. R. Andersson, J. Chem. Phys. **115**, 7235 (2001).
[22] E. A. Katz, D. Faiman, S. M. Tuladhar, J. M. Kroon, M. M. Wienk, T. Fromherz, F. Padinger, C. J. Brabec, and N. S. Sariciftci, J. Appl. Phys. **90**, 5343 (2001).
[23] J. Nelson, Phys. Rev. B **67**, 155209 (2003).
[24] H. J. Snaith, A. C. Arias, A. C. Morteani, C. Silva, and R. H. Friend, Nano Lett. **2**, 1353 (2002).
[25] J. Kroom, M. Wienk, W. Verhees, and J. Hummelen, Thin Solid Films **403-404**, 223 (2002).
[26] M. Yan, L. J. Rothberg, F. Papadimitrakopoulos, M. E. Galvin, and T. M. Miller, Phys. Rev. Lett. **72**, 1104 (1994).
[27] E. Frankevich, H. Ishii, Y. Hamanaka, T. Yokoyama, A. Fuji, S. Li, K. Yoshino, A. Nakamura, and K. Seki, Phys. Rev. B **62**, 2505 (2000).
[28] J. G. Müller, U. Lemmer, J. Feldmann, and U. Scherf, Phys. Rev. Lett. **88**, 147401 (2002).
[29] C. Waldauf, W. Graupner, S. Tasch, G. Leising, A. Gugel, U. Scherf, A. Kraus, M. Walter, and K. Müllen, Opt. Mater. (Amsterdam, Neth.) **9**, 449 (1998).
[30] C. J. Brabec, F. Padinger, N. S. Sariciftci, and J. C. Hummelen, J. Appl. Phys. **85**, 6866 (1999).
[31] D. Hertel, U. Scherf, and H. Bässler, Adv. Mater. (Weinheim, Ger.) **10**, 1119 (1998).
[32] W. Geens, S. E. Shaheen, B. Wessling, C. J. Brabec, J. Poortmans, and N. S. Sariciftci, Org. Electron. **3**, 105 (2002).
[33] Due to a larger thickness of our MDMO-PPV:PCBM devices the photocurrent is somewhat lower than usually reported for this material combination.
[34] L. Rothberg, M. Yan, A. Fung, T. Jedju, E. Kwock, and M. Galvin, Synth. Met. **84**, 537 (1997).
[35] C. Zenz, G. Lanzani, G. Cerullo, W. Graupner, G. Leising, and S. DeSilvestri, Chem. Phys. Lett. **341**, 63 (2001).
[36] A. Haugeneder, M. Neges, C. Kallinger, W. Spirkl, U. Lemmer, J. Feldmann, M. C. Amann, and U. Scherf, J. Appl. Phys. **85**, 1124 (1999).
[37] G. Cerullo, S. Stagira, M. Nisoli, S. De Silvestri, G. Lanzani, G. Kranzelbinder, W. Graupner, and G. Leising, Phys. Rev. B **57**, 12806 (1998).
[38] W. Graupner, G. Cerullo, G. Lanzani, M. Nisoli, E. J. W. List, G. Leising, and S. De Silvestri, Phys. Rev. Lett. **81**, 3259 (1998).
[39] The strongest absorption of charge-induced absorption has been found at 1.24 eV. At this spectral position, however, triplet absorption obscures the results (Ref. 40).
[40] G. Zerza, M. C. Scharber, C. J. Brabec, N. S. Sariciftci, R. Gomez, J. L. Segura, N. Martin, and V. I. Srdanov, J. Phys. Chem. A **104**, 8315 (2000).
[41] A. Haugeneder, M. Neges, C. Kallinger, W. Spirkl, U. Lemmer, J. Feldmann, U. Scherf, E. Harth, A. Gugel, and K. Müllen, Phys. Rev. B **59**, 15346 (1999).
[42] J. M. Lupton, Appl. Phys. Lett. **80**, 186 (2002).
[43] C. Silva, A. S. Dhoot, D. M. Russell, M. A. Stevens, A. C. Arias, J. D. MacKenzie, N. C. Greenham, R. H. Friend, S. Setayesh, and K. Müllen, Phys. Rev. B **64**, 125211 (2001).
[44] C. Gadermaier, G. Cerullo, G. Sansone, G. Leising, U. Scherf, and G. Lanzani, Phys. Rev. Lett. **89**, 117402 (2002).
[45] P. V. Kamat, J. Am. Chem. Soc. **113**, 9705 (1991).
[46] B. Kraabel, J. C. Hummelen, D. Vacar, D. Moses, N. S. Sariciftci, A. J. Heeger, and F. Wudl, J. Chem. Phys. **104**, 4267 (1996).
[47] B. Schweitzer, V. I. Arkhipov, U. Scherf, and H. Bässler, Chem. Phys. Lett. **313**, 57 (1999).
[48] V. I. Arkhipov, E. V. Emelianova, and H. Bässler, Chem. Phys. Lett. **372**, 886 (2003).
[49] T. Offermans, S. C. J. Meskers, and R. A. J. Janssen, J. Chem. Phys. **119**, 10924 (2003).
[50] J. Cornil, D. A. dos Santos, X. Crispin, R. Silbey, and J. L. Bredas, J. Am. Chem. Soc. **120**, 1289 (1998).
[51] F. Schindler, J. M. Lupton, J. Feldmann, and U. Scherf, Proc. Natl. Acad. Sci. U.S.A. **101**, 14695 (2004).
[52] J. M. Lupton, Chem. Phys. Lett. **365**, 366 (2002).
[53] B. Valeur, *Molecular Fluorescence* (Wiley-VCH Verlag, Weinheim, Germany, 2002).
[54] J. G. Müller, J. M. Lupton, J. Feldmann, U. Lemmer, and U. Scherf, Appl. Phys. Lett. **84**, 1183 (2004).
[55] D. Beljonne, G. Pourtois, C. Silva, E. Hennebicq, L. M. Herz, R. H. Friend, G. D. Scholes, S. Setayesh, K. Müllen, and J. L. Bredas, Proc. Natl. Acad. Sci. U.S.A. **99**, 10982 (2002).
[56] J. G. Müller, U. Lemmer, G. Raschke, M. Anni, U. Scherf, J. M. Lupton, and J. Feldmann, Phys. Rev. Lett. **91**, 267403 (2003).